IOP Publishing Superconductor Science and Technology
Supercond. Sci. Technol. 31 (2018) 105007 (11pp) https://doi.org/10.1088/1361-6668/aad78a

Magnetizing high-T_c superconducting coated conductor stacks using a transformer–rectifier flux pumping method

Heng Zhang, Jianzhao Geng and T A Coombs

Department of Engineering, University of Cambridge, Cambridge, CB3 0FA, United Kingdom

E-mail: jg717@cam.ac.uk

Received 14 May 2018, revised 23 July 2018
Accepted for publication 2 August 2018
Published 31 August 2018

Abstract

High-T_c superconducting (HTS) coated conductor stacks have been demonstrated as very promising superconducting permanent magnets (PMs), to be used in applications like rotary motors and levitation devices. In this paper, we present a novel magnetization method to address a key problem in the application of HTS stacks, which is effective magnetization with compact, light and efficient setups. The proposed method, transformer–rectifier flux pumping, uses the mechanism developed for HTS coils to magnetize the modified HTS stacks. The accumulation of flux with time is achieved in the HTS stacks. The results show that the flux pump can effectively magnetize long HTS stacks with a magnetic field applied to a much smaller area. Operational characteristics of the flux pump are experimentally studied and some explanations are proposed for the distinct behaviors observed in the experiments. This study heralds a new direction in the magnetization of superconducting PMs and has the potential to be a practical method for industrial applications.

Keywords: flux pumping, stacked tape, transformer–rectifier, HTS

(Some figures may appear in colour only in the online journal)

1. Introduction

HTS bulks are able to trap a large magnetic flux via the generation of persistent macroscopic currents within the grains. Extensive studies on the flux trapping of HTS bulks show their ability to provide a large magnetic field from a compact source is unparalleled [1–3]. This property makes HTS bulks highly attractive for replacing permanent magnets (PMs) or some electromagnets in a variety of engineering applications, such as magnetic levitation [4, 5], magnetic bearing [6] and rotating machines [7]. These type of superconductors are called trapped field magnets or superconducting PMs. The compactness and high flux-trapping capability of superconducting PMs enable rotating machines to be made with a high power density, which is highly desirable in applications like MW-class wind turbines and ship propulsion motors. However, HTS bulks suffer from thermal instability at lower temperatures (<30 K), due to the low thermal conductivity of superconductors and the inhomogeneity in critical current density J_c, preventing the large flux-trapping potential of the HTS bulks from being exploited [8]. HTS bulks also require external mechanical reinforcement, typically a steel ring [3], when carrying large magnetization currents, as a result of their relatively poor mechanical strength. In the operation of practical applications, a major concern is the demagnetization of superconducting PMs caused by an external ac magnetic field orthogonal to the original magnetization direction, called a cross-field [9]. The decay in magnetization in HTS bulks can be significant, reducing the magnetization by 50% with only one cross-field cycle when its direction is perpendicular to the original magnetization, with the magnitude close to the trapped field intensity [9].

A stack of commercial HTS coated conductor tapes can also be employed as a superconducting PM once magnetized [10–13]. The relatively uniform J_c in HTS stacks and the much higher thermal conductivity of the silver over-layers in coated conductor tapes give HTS stacks a more superior

thermal stability than bulks. Also, the metallic substrates in the HTS tapes give a much stronger mechanical strength than bulks. A remarkable field trapping ability of HTS stacks was reported by Patel *et al* [14–16], with a trapped field of 2 T at 10 K using pulsed field magnetization (PFM) [14] and over 17 T at around 4.2 K using field cooling (FC) [16]. Baghdadi *et al* [17] reported a significantly reduced demagnetization in pre-magnetized HTS stacks under a cross-field, showing a much better cross-field performance than bulks. The superior mechanical and thermal properties, and the much lower demagnetization under a cross-field, make HTS stacks a good alternative to HTS bulks and a promising candidate for superconducting PMs for engineering applications.

However, a major difficulty of using superconducting PMs in practical applications is in the magnetization process (field trapping process). There are three types of magnetization techniques for trapped field magnets: FC, zero field cooling (ZFC) and PFM. Assuming Bean's model [18], the magnitude of the applied field required is at least twice the trapped field B_{trap} for ZFC and at least B_{trap} for FC, and the area of the applied field should cover the whole HTS sample to achieve the above result. This inevitably results in large and heavy magnetization setups and makes it particularly impractical on most of the applications where magnetization *in situ* is essential. PFM, which is essentially pulsed ZFC when reducing the field application time from many minutes to milliseconds, is currently the most practical and economical magnetization method for superconducting PMs. PFM can also effectively reduce the field magnitude requirement if a flux jump is triggered [19]. However, the rapid flux penetration of pulsed fields gives rise to a temperature increase in the samples, which causes the J_c degradation and leads to much smaller trapped fields than FC and ZFC. As a result, the benefits of using superconducting PMs are seriously compromised.

We proposed using the traveling-field based flux pumping method [20–24] developed for HTS bulks and coils to magnetize modified HTS stacks in our previous work [25]. The proposed methods aim to magnetize the superconducting PMs in a gradual manner with a smaller applied field, rather than an one-off process as in conventional magnetization techniques. Each layer of the HTS stack is transformed into a flat single-turn coil with slits created in the middle of the tapes. This modification aims to employ the quasi-dc voltage created by the HTS flux pump to energize each layer of the stack as in the HTS coils. However, although a flux pumping effect was observed, the performance of the travelling-wave flux pump on the stacks was far from satisfactory.

In this paper, we investigate using a transformer–rectifier flux pump to magnetize HTS stacks. Although this flux pump developed by Geng *et al* [26] was originally for charging HTS coils, we will show that through improved design the flux pump is suitable for magnetizing HTS stacks.

2. Flux pumping mechanism, stack modification, and experimental system

2.1. Mechanism of the transformer–rectifier flux pump

There are two closed superconducting loops in the circuit of the transformer–rectifier flux pump for HTS coils: the closed loop of the HTS coil, which is called the load loop, and another loop formed by a closed HTS tape called the charging loop. The charging loop is wound around an iron core as the secondary winding of a transformer. The common part of the two loops is called the bridge. Alternating transport current i_P is induced in the charging loop by the transformer. This current initially flows through the bridge. An ac magnetic field with a frequency higher than i_P is intermittently applied on the bridge perpendicular to the tape face when the bridge current is positive. The applied field triggers a net flux flow in the current-carrying bridge superconductor, allowing flux to accumulate in the load loop. The flux motion effect can also be understood as a dynamic resistance, which occurs when a dc carrying a type II superconductor is subjected to a perpendicular ac field [27–30]:

$$R_{dyn} = \frac{2afl}{I_c}(B_a - B_{a,th}) \tag{1}$$

where a is the width of the tape, l is the length of the tape under the applied field, f and B_a are the frequency and amplitude of the applied ac field respectively, I_c is the critical current of the tape and $B_{a,th}$ is the threshold value [28–30]. The flux transfer from the charging loop to the HTS coil is associated with a dc voltage developed across the dynamic resistance on the bridge. The equivalent circuit diagrams are shown in figure 1(a) for the circuit with the applied field and in figure 1(b) without the applied field, in which the HTS coil is represented by an inductance L and a resistance R_L. One equivalent resistance R_1 is shown in the charging loop to represent the loss caused by flux penetration during the induction of i_P as well as the joint resistance in the charging loop. The resistance R_1 is essential for the flux pump to work [31]. It enables the flux to link the charging loop from outside. Without the resistance R_1, the sum of the flux linking the charging loop and the load loop is conservative, the flux increase in the load loop is accompanied by a flux decrease in the charging loop, and an increasing dc current bias will occur in the charging loop. The existence of R_1 limits the current bias in the charging loop. The load current i_L can be predicted as the current response in a series RL circuit connected to a dc voltage source given by:

$$V_0 = R_{dyn}(i_P - i_L). \tag{2}$$

The maximum current injected to the coil is given by [25]:

$$I_L = \frac{I_P}{1 + \frac{R_L}{R_{dyn}p}} \tag{3}$$

where I_P is the average value of i_P experiencing the applied field, and p is the duty cycle defined by the ratio of bridge field application time to the period of i_P.

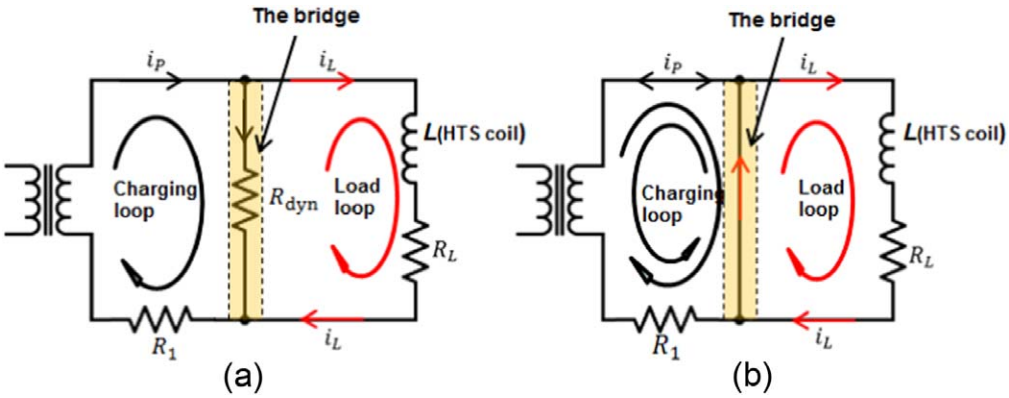

Figure 1. The equivalent circuit for the transformer–rectifier HTS flux pump for HTS coils when the bridge field is applied (a) and turned off (b).

2.2. Modification of the HTS stack and the experimental system

Although the above mentioned flux pumping mechanism has been successfully applied to magnetize HTS coils, for magnetizing HTS stacks, some modifications are necessary. The two-loop superconducting circuit in a stack is created by cutting slits in the middle of the tape in each layer. The slits produce insulating barriers to force the currents to flow in the designed paths of the loops, however the trapped field profile of the HTS stack is not considerably changed by the slits. Figure 2(a) is the schematic drawing of a single superconducting layer with two slits. Two fully superconducting loops are formed in the tape with a gap between two slits as the bridge region, denoted as the 1st loop for the charging loop and the 2nd loop for the load loop (the 2nd loop may be much larger than the 1st loop in terms of size and inductance). Currents can flow separately in the 1st loop and the 2nd loop, and share the path in the bridge area. Our aim is to magnetize the 2nd loop by applying fields in the 1st loop and the bridge area. Figure 2(b) shows the top view and side view of a stack of tapes with slits.

The HTS tapes used in the experiment are the 12 mm SCN12600 copper stabilized tapes supplied by SuNam, which have the minimum critical current of 600 A at 77 K and self-field. The length of the HTS stack is 200 mm with the 1st loop being 50 mm (including the bridge width = 8 mm), and the 2nd loop being 150 mm. The slits are made by the multiple passing of a utility knife and the loss of the superconducting tape width is estimated to be 20%.

Two electromagnets with gapped iron cores are designed to apply the fields on the 1st loop and on the bridge. As shown in figure 3, the cross section of the 1st magnet at the air gap is wider than the tape width (12 mm) and can cover a large portion of the 1st loop in length, and the cross section of the 2nd magnet is designed to be variable by changing the number and width of the soft iron plates. The currents in windings of the electromagnets are supplied from two individual power supplies, namely a Kepco Bop for the 1st magnet and an Europower power amp for the bridge magnet, controlled by a LabVIEW program via a National Instruments digital-to-analog converter. In this setup, the 1st magnet acts as a transformer, in which the 1st superconducting loop is its secondary.

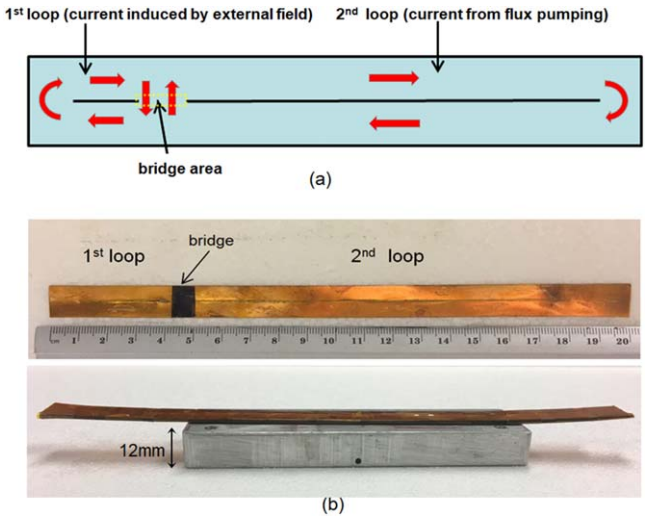

Figure 2. The modified tape stack. (a) A tape with two slits in the middle, forming two current loops, the smaller 1st loop is for inducing circulating current, and the larger 2nd loop is the magnet we want to magnetize. The two loops share a common current path, called the bridge (the yellow dotted enclosed area). (b) Top view and side view of the experimental HTS stack with slits, with the bridge painted in black.

To monitor the induced circulating current in the 1st loop, a pre-calibrated Hall probe is placed on the slit of the HTS stack top surface in their 1st loops, between the 1st magnet and the 2nd magnet. The interference in the measured field from the fringing fields produced by the 1st magnet and the 2nd magnet is eliminated by pre-calibration and operations in LabVIEW. Another Hall probe is placed on the slit of the stack top surface in the 2nd loop to measure the field trapped with flux pumping, at a position where the fringing field from the electromagnets and the end effect is considered negligible. As shown in figure 3, the HTS stack and the lower parts of the magnets are immersed in a liquid nitrogen bath.

3. Experiment and preliminary result

A triangular alternating magnetic field of 0.5 Hz is generated by the 1st magnet. The peak value of the field is manually

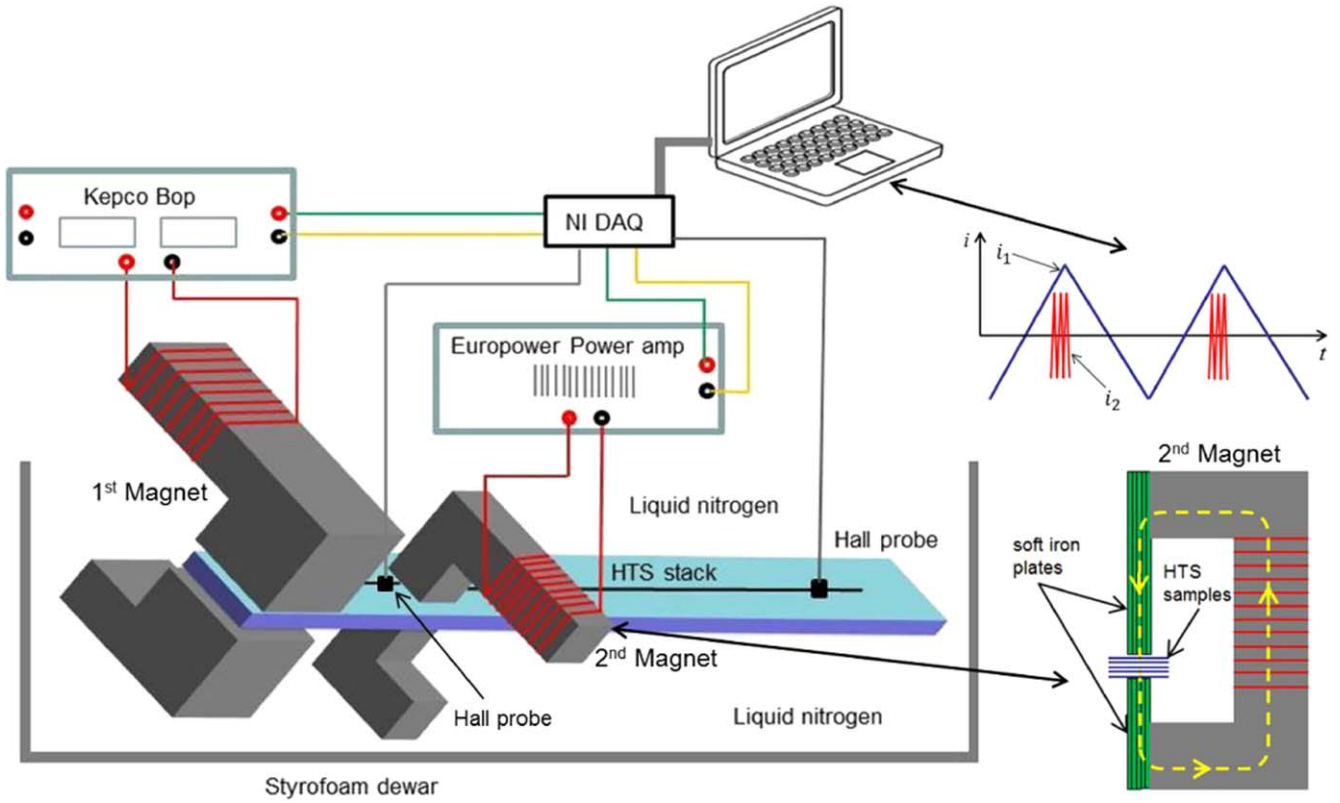

Figure 3. The schematic drawing of experimental rig of the rectifier-type flux pump for magnetization of HTS stacks.

altered to use the smallest field to induce the critical current of the 1st loop. This is achieved by finding the maximum peak–peak value without a flat-top in the trapped field waveform measured by the Hall probe on the 1st loop. For all of the experiments in this study, the peak value of the 1st loop current i_P is adjusted to its critical current. A sinusoidal bridge field was applied by the 2nd magnet around the positive peaks of i_P. The bridge field has a frequency of 30 Hz, the magnitude of 275 mT and the duty cycle of 5% which stands for three complete bridge field cycles in each cycle of i_P. The two signals are synchronized by programming in LabVIEW, which has been reported in our previous work [26].

Figure 4 shows the field measured on the top surface of the 2nd loop of a stack of four tapes. A flux pumping curve similar to the results for an HTS coil in [26] is observed. The flux pump operates in a bipolar manner in which the pumping direction reverses when the bridge field is applied on the opposite peaks of i_P. One can see three sharp peaks in the waveform of figure 4(c) between two cycles of i_P, which are induced by the three cycles of bridge fields leading to the magnitude increase in the trapped field of the 2nd loop. However, the pumping curve is much less smooth than the one for coils as it is interrupted by sharp peaks induced by the bridge field. This is due to strong mutual coupling between the two loops of the stack.

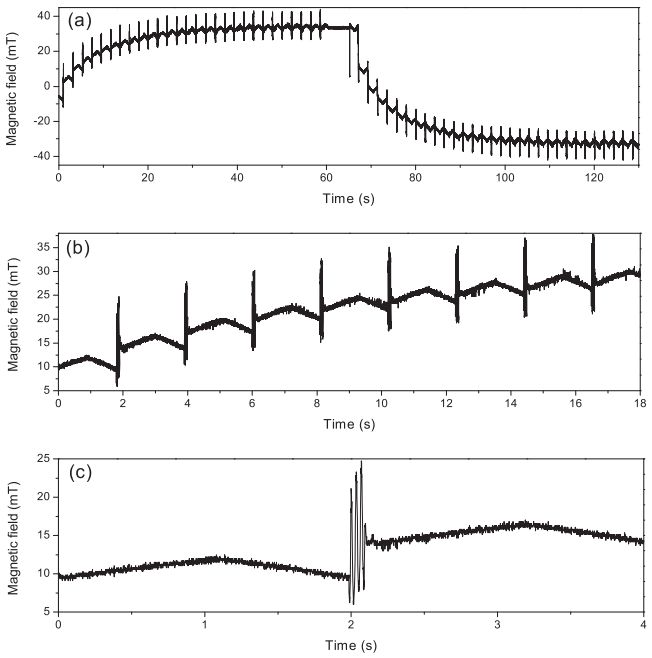

Figure 4. Field measured on the top surface of the 2nd loop of the four-layer HTS stack under the bridge field magnitude of 275 mT, 30 Hz. (a) The whole charging curve showing positive charging and negative charging. (b) Detail of the charging curve showing several cycles. (c) Charging detail in one ac cycle, showing the load current increase after ac field is applied.

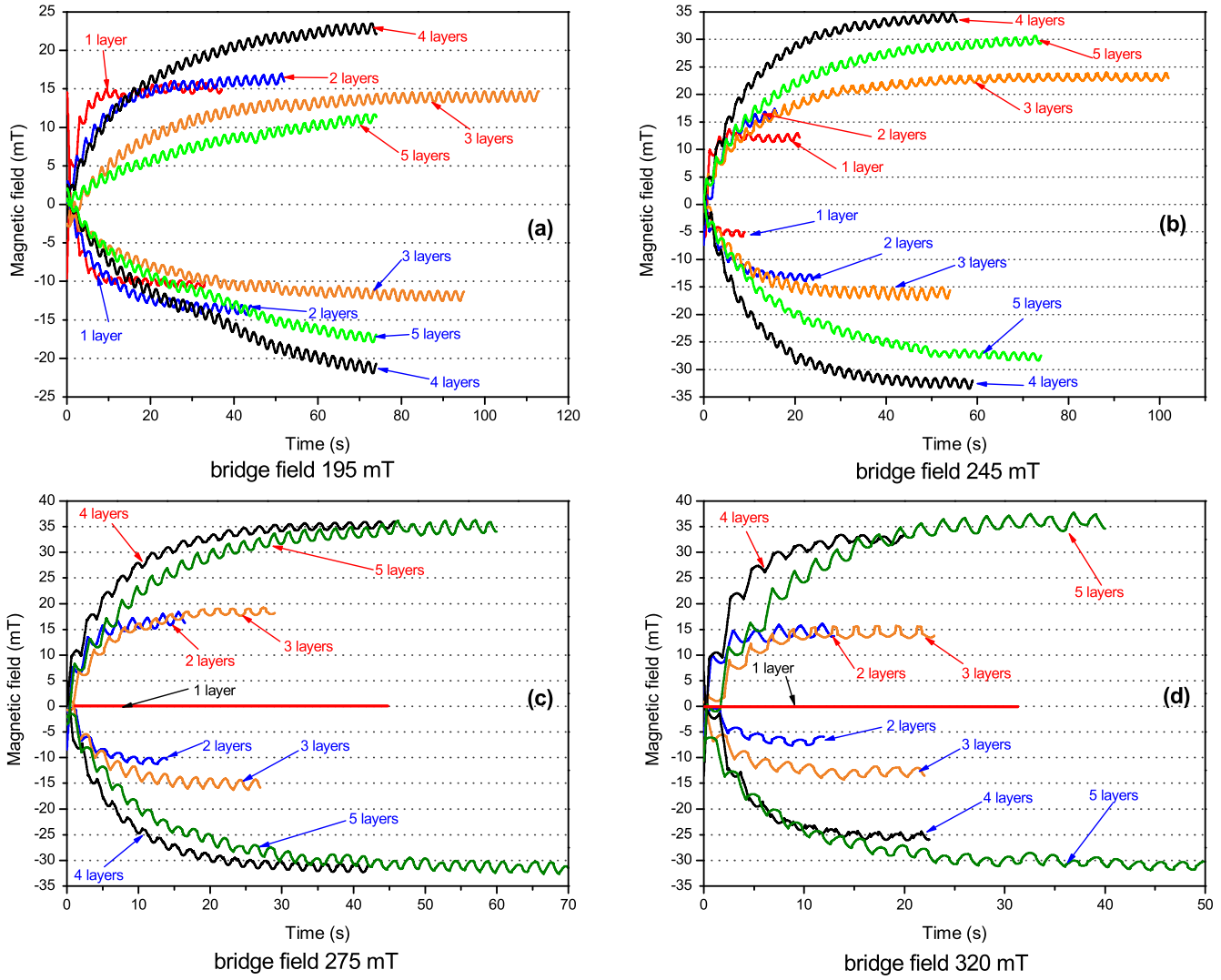

Figure 5. Flux pumping results for the stack of one, two, three, four and five layers under the bridge field magnitudes of (a) 195 mT, (b) 245 mT, (c) 275 mT and (d) 320 mT. The bridge field is applied at the positive peaks and then the negative peaks of the 1st loop current to achieve flux pumping in opposite directions.

HTS stacks with different numbers of layers are used and the bridge field magnitude is varied to study the flux pumping performance under different bridge fields. The results are shown in figure 5 for a stack of one, two, three, four and five layers under bridge fields of 195 mT, 245 mT, 275 mT and 320 mT. Flux pumping is performed in both directions with the bridge field applied on the opposite peaks of the 1st loop current, and both fields are applied with perfect symmetry in two directions. The results are recorded until no increase in the trapped field is observed for more than 20 s. Therefore, the pumping curves are able to show the maximum pumped field in the 2nd loop under the current conditions.

However, the pumping results in figure 5 show some interesting features which are unexpected and fairly different from the experimental results for HTS coils [32]. A higher bridge field does not always lead to higher pumped fields. This feature is clearly shown with the comparison between the one-layer stack and the five-layer stack under four different bridge fields, in which the five-layer stack has a better pumping performance under higher bridge fields (275 mT, 320 mT) than lower fields (195 mT, 245 mT), however the opposite effect of bridge field magnitude is observed for the single-layer tape. More layers in the stack can sometimes cause a lower pumped field, especially under lower bridge fields.

To understand the distinct features of flux pumping performance on the HTS stacks and to further explore the operational characteristics, we proposed an analytical model to explain and predict flux pumping performance, together with experimental studies on the influence of different factors in the model on pumping performance. This is presented in the following section.

4. Operational study and analysis

4.1. Proposed equivalent circuit model for HTS stacks

Two fully superconducting loops in the HTS stacks allow us to eliminate the load resistance caused by joint resistance in

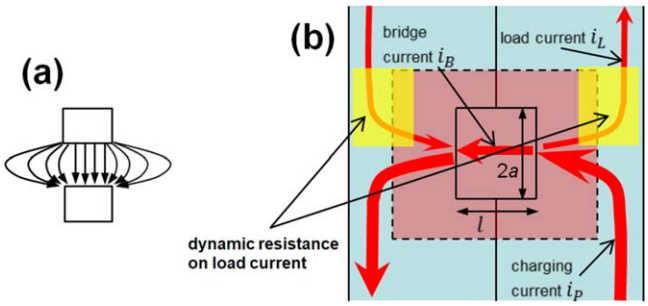

Figure 6. (a) The field in the air gap between the magnets covers a much larger area than the magnet cross section due to the fringing effect. (b) Schematic illustration of the dynamic resistance produced on the load currents by the bridge leakage field.

the equivalent circuit. However, an increased bridge field sometimes leads to a lower final pumped field, which is in contrast to the results for HTS coils as a larger dynamic resistance can be triggered with a larger bridge field and therefore lead to larger current injection as described by equation (3). We attribute this to the extra loss induced by the leakage field from the 2nd magnet on the 2nd loop. Because the cross section of the 2nd magnet is narrow, and the bridge superconductor expels the flux lines, the field strays to an adjacent area of the bridge, rather than being merely perpendicular to the air gap. A large leakage ac magnetic field may trigger dynamic resistance in the 2nd loop. Dynamic resistance on the bridge is the origin of the quasi-dc voltage for flux pumping. However, dynamic resistance on the load current is dissipative leading to current decay. The dynamic resistance on the load current (2nd loop current) is illustrated in figure 6, in which the cross section of the 2nd magnet on the bridge is shown by the rectangular area with length $2a$ and width l. However, the actual area subject to the bridge field is much larger than the magnet cross section, as depicted with the rectangular area surrounded by broken lines. Therefore, the equivalent circuit for the flux pump on HTS stacks is presented in figure 7, in which the load resistance R_L stands for the dynamic resistance on the 2nd loop current and is only present when the bridge field is applied. When the bridge field is switched off, the 2nd loop is in a persistent mode with no flux flow, neither positive nor negative.

The flux transferred from the 1st loop to the 2nd loop in each cycle of i_P, denoted by T, is given by:

$$\Delta\Phi = \int_0^{pT} L\frac{di_L}{dt}dt = (I_P - i_L)R_{dyn}pT - i_L R_L pT. \quad (4)$$

When T is very small compared with the total charging time, one arrives at the charging rate of the flux pumping process:

$$\frac{\Delta\Phi}{T} = pL\frac{di_L}{dt} = I_P R_{dyn}p - i_L(R_{dyn}p + R_L p). \quad (5)$$

And the maximum injected current can be obtained with the solution to $\frac{\Delta\Phi}{T} = 0$, which is given as below:

$$I_L = \frac{I_p}{(1 + R_L/R_{dyn})}. \quad (6)$$

It can be seen from equation (6) that the maximum current injected is determined by the ratio of the dynamic resistances on the 2nd loop and on the bridge, and is unrelated to the duty cycle p and bridge field frequency f as R_L and R_{dyn} are triggered by the same bridge field. Figure 8 shows the experimental results for the one-layer and two-layer stacks under bridge fields of 30 Hz, 60 Hz and 90 Hz, of the magnitude of 170 mT for the one-layer stack and 275 mT for the two-layer stack. It suggests the bridge field frequency does not influence the maximum pumped field much, in contrast to the behaviour for HTS coils shown in [32] in which a higher field is pumped with a higher frequency. This is because the origin of load resistance R_L in HTS coils is the joint resistance, which is independent of frequency.

As shown in equation (6), a lower ratio of R_L/R_{dyn} is desirable for a larger final pumped field. The ratio R_L/R_{dyn} is primarily affected by the magnitude of the bridge field and the cross section area of the 2nd magnet. As described in equation (1), dynamic resistance can only be triggered when the threshold value $B_{a,th}$ is exceeded by the applied field B_a. It is usually more difficult to exceed the threshold value $B_{a,th}$ on the 2nd loop than on the bridge, due to its larger distance to the 2nd magnet. We can assume at some smaller fields that only the dynamic resistance on the bridge is triggered and $R_L/R_{dyn} = 0$. In contrast, R_L/R_{dyn} can rise to a significant level when the bridge field is sufficiently large, triggering large dynamic resistances on both the bridge and the 2nd loop. Therefore, the ratio R_L/R_{dyn} is expected to increase with increased bridge field.

R_L/R_{dyn} can also be increased by increasing the width l of the 2nd magnet cross section, which shortens the distance between the 2nd loop current and the 2nd magnet, therefore making it easier to trigger and increas R_L. One arrives at the conclusion that a smaller bridge field intensity and 2nd magnet cross section can lead to a better pumping performance as long as the dynamic resistance on the bridge field is successfully triggered.

4.2. Influence of the screening effect

Screening currents are induced in HTS tapes when they are subject to an external magnetic field, which tends to shield the applied field. As a result, the inner layers of a stack are subject to much a weaker external field than the outer layers. As for the flux pump, the bridge field seen by the inner layers is much smaller and leads to weaker flux pumping. If flux pumping does not occur in one specific layer of the stack, the 2nd loop of this layer acts as a shield for the trapped field in other layers due to its diamagnetic nature, and reduces the overall trapped field. This possibly explains why a smaller total pumped field is observed in a stack with more layers. A similar screening effect has been shown in [33], where the

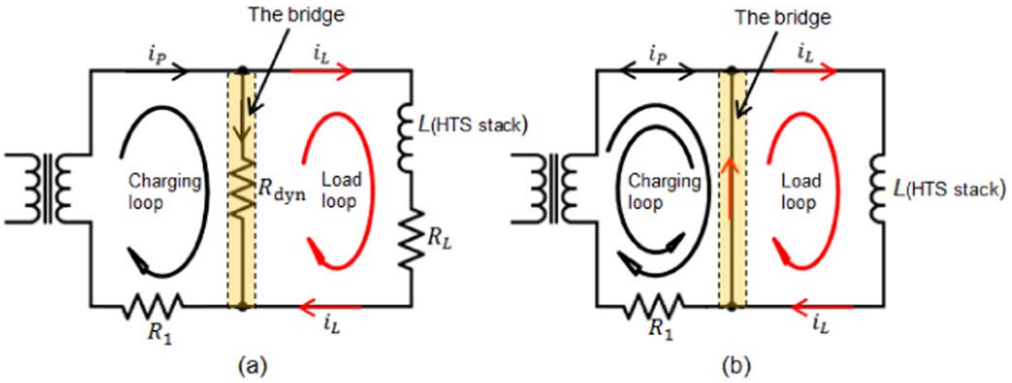

Figure 7. The equivalent circuit for the rectifier-type flux pump for HTS stacks, when the bridge field is applied (a) and turned off (b).

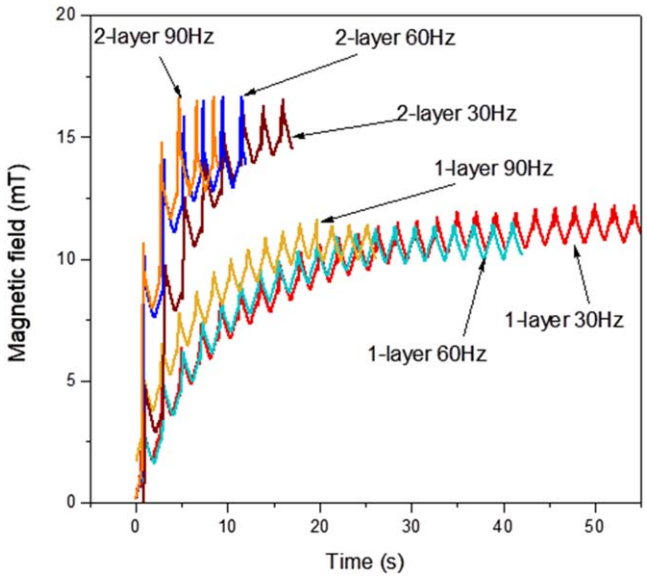

Figure 8. Flux pumping results of the one-layer stack and two-layer stack under a bridge field of different frequencies (30 Hz, 60 Hz and 90 Hz). The bridge field magnitude is 170 mT for the one-layer stack, and 275 mT for the two-layer stack.

dynamic resistance of a four-layer stack was measured, and a higher threshold field was observed in a four-layer stack than in a single tape. The screening effect is more significant when the area and geometry of the tapes allow a larger screening current to flow, namely a higher shielding capability. As depicted in figure 9, the maximum screening current at the bridge is defined by the gap between two slits when the gap is smaller than the tape width. However the applied flux on the bridge is primarily defined by the 2nd magnet cross section and the bridge field intensity. It is much easier to screen the applied flux if the area allowed for the screening current is much larger than the 2nd magnet cross section. Therefore, a larger magnet cross section or larger field intensity is preferred to minimize the screening effect in the middle layers.

One can see that this leads to a design preference contradictory to the previous discussion intending to minimize R_L/R_{dyn} through reducing the 2nd magnet cross section and the bridge field intensity. Both the screening effect and the dynamic resistance on the 2nd loop (R_L) result in a

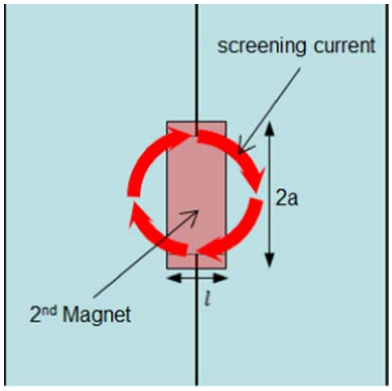

Figure 9. Schematic illustration of the maximum screening current at the bridge region defined by the distance between two slits, in comparison with the area of the bridge magnet.

degradation of the pumping performance. Nevertheless, the methods of reducing them are opposite and the two effects may appear counterbalancing. At present, the influence of each effect cannot be precisely predicted due to the lack of a quantitative model. Instead, we study these effects experimentally. Three factors are varied in the experiments: the width l of the 2nd magnet cross section, the bridge field intensity and the number of layers in a stack. The experimental results are presented in the following section.

4.3. Experiments on the influence of R_L/R_{dyn} and the screening effect on pumping performance

To allow larger screening currents to flow in the bridge region of each layer, the gap between two slits is enlarged to 10 mm. The width l of the 2nd magnet cross section is varied to be 1 mm, 2 mm and 3 mm by changing the number of soft iron plates. The one-layer, three-layer and five-layer HTS stacks are under bridge fields of 195 mT, 245 mT, 275 mT and 320 mT and the results are shown in figure 10.

It can be seen from the results for the one-layer stack that a smaller bridge field and smaller cross section width leads to a higher pumping performance. In contrast, for the five-layer stack, a higher bridge field (275 mT, 320 mT) results in better pumping than lower fields (195 mT, 245 mT), and almost no flux pumping was observed at 195 and 245 mT when the 2nd

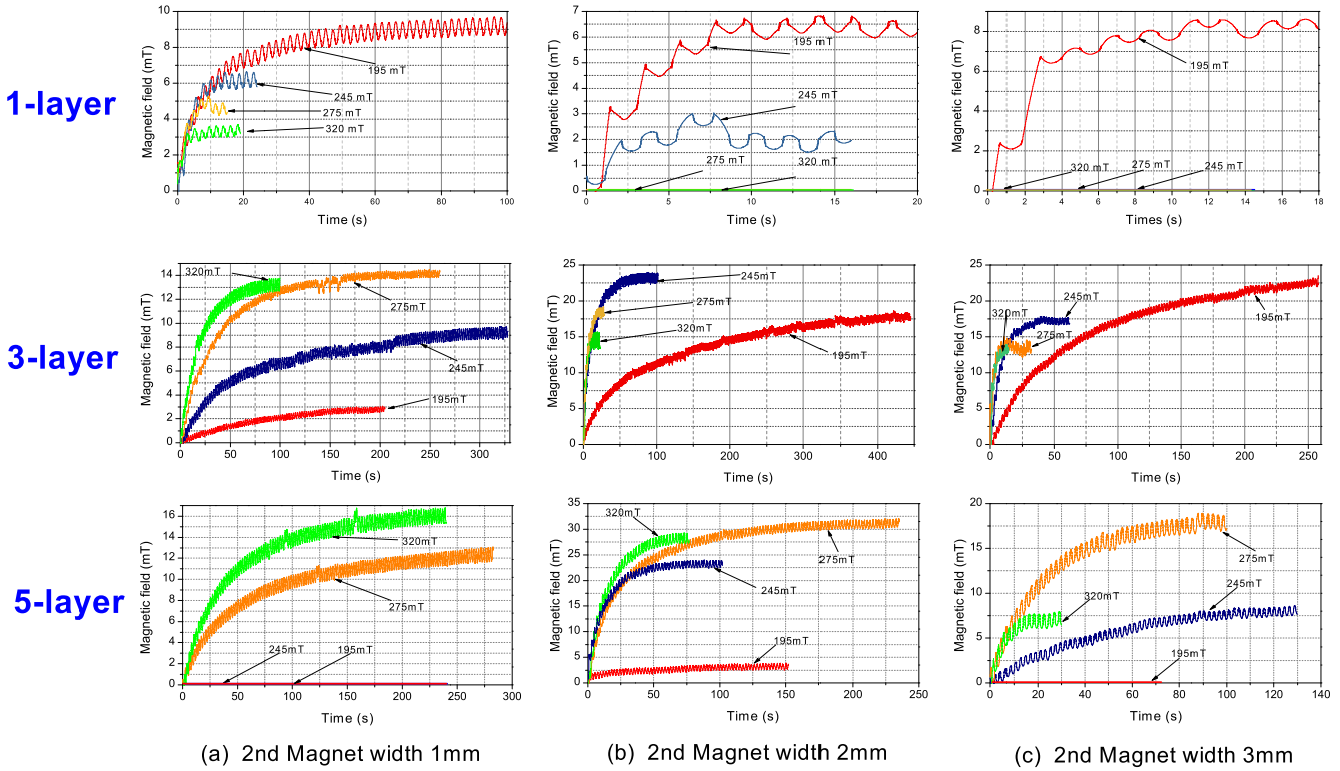

Figure 10. Flux pumping results for the one-layer, three-layer and five-layer stacks under bridge fields of 195 mT, 245 mT, 275 mT and 320 mT, using the 2nd magnet with widths of 1 mm, 2 mm and 3 mm.

magnet was thin ($l = 1$ mm). Obvious flux pumping occurs at 245 mT, 275 mT and 320 mT when the width of the 2nd magnet is increased to 2 mm, and the maximum pumped field of 32 mT for the five-layer stack is reached with a bridge field of 275 mT. However, flux pumping weakens when the magnet width is further increased to 3 mm where the pumped field under the bridge field of 320 mT drops to below $1/3$ of that of the 2 mm magnet. This implies extra loss caused by the large dynamic resistance on the load currents produced by the leakage bridge field. The most evident example is the three-layer stack, in which the rank of pumped field under different bridge fields almost reverses when the width of the 2nd magnet is increased from 1 mm to 3 mm.

The comparison between the stacks with different number of layers verifies that a stack with more layers favors a larger magnet width and bridge field intensity, to overcome the large screening effect in the multi-layer structure. However, the bridge field intensity and the magnet cross section still need to be limited to avoid the extra loss induced on the 2nd loop. To achieve optimal performance requires the consideration of three factors in the flux pump design, which can only be achieved by trial and error at this stage.

4.4. Improved pumping performance with shielding layers

The loss in the 2nd loops of the HTS stacks can be reduced if the impact of the bridge leakage field on the load current is reduced below certain values. The key is to ensure that dynamic resistance is effectively triggered in the bridge, but

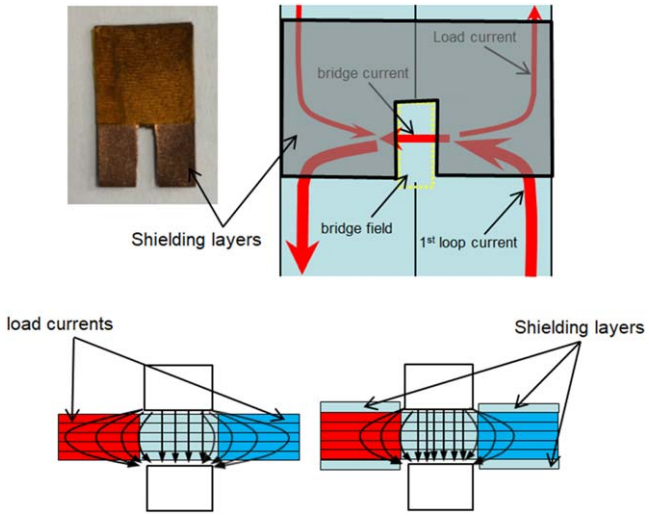

Figure 11. Superconducting shielding layers are attached to the top and bottom layers of the stack at the bridge area, which can reduce the fringe field thus suppressing the dynamic resistance of load currents.

suppressed in the load currents. The difficulty lies in the fact that there is no clear boundary between the bridge region and the load region for this specific geometry. The position of the boundary changes as the flux pumping progresses. Further study is required to understand the current distribution in the geometry during the flux pumping process. This will provide important information for the design of flux pumps to minimize the loss on the load loops caused by the bridge field.

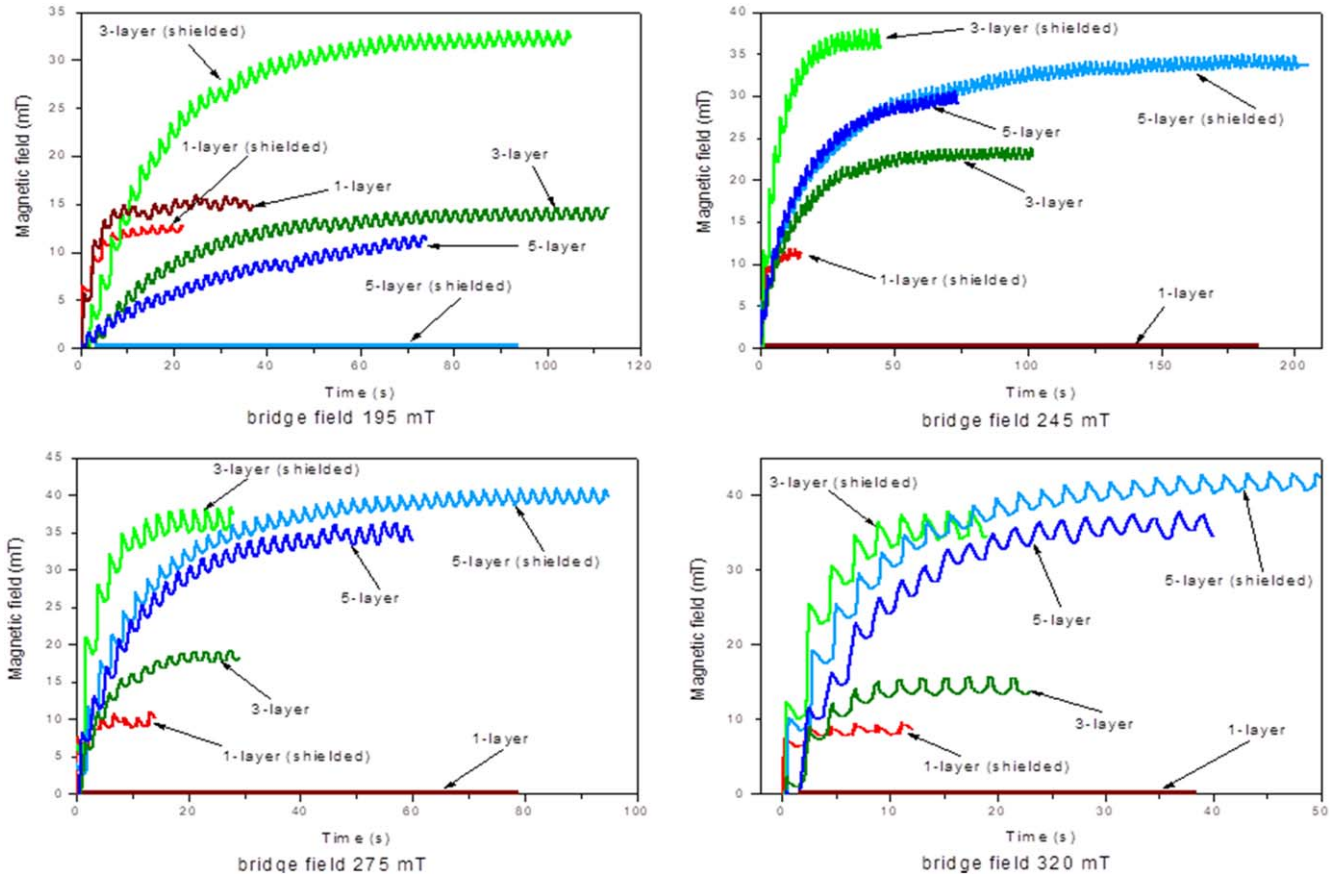

Figure 12. Flux pumping results for the HTS stacks of one, three and five layers with and without shielding layers under bridge fields of 195 mT, 245 mT, 275 mT and 320 mT. It is clear that the shielding layer can improve the maximum pumped current.

Adding superconducting layers on the load regions close to the bridge may have a shielding effect on the bridge field. The increased thickness of the load loops increases the threshold value, $B_{a,\,th}$, making it more difficult to trigger dynamic resistance on the load currents by the bridge field. The shielding layers are illustrated in figure 11. A small number of shielding layers can significantly increase the threshold value of the load loops. Without transport current flowing in the shielding layers, the bridge field has to overcome the penetration field, H_p, of the shielding layers to trigger the dynamic resistances in the layers underneath.

Experiments were performed to show the effect of the shielding layers. The gap between two slits was 8 mm and the pumping result is compared with the results without shielding layers extracted from figure 5. The pumping results are shown in figure 12 for the one-layer, three-layer and five-layer stacks with two shielding layers added both on the top and bottom of the stacks, under bridge fields of 195 mT, 245 mT, 275 mT and 320 mT. The pumping performance is clearly improved by the shielding layers, especially for stacks with fewer layers (one-layer and three-layer) where the dynamic resistance on the load currents is much easier to trigger. Significant flux pumping can be observed on the one-layer stack with shielding layers, which is almost non-existent without the shielding layers under higher bridge fields (245 mT, 275 mT, 320 mT).

5. Further discussion

The transformer–rectifier flux pump is able to charge HTS coils to, or even slightly over, their critical current. In contrast, in the stacked tape case, the final pumped load field is less than half of the fully penetrated field of the stack in all experiments. One reason is that the slit in the load reduced the current capacity of the tape, and the maximum circulating current the tape can carry is limited by the narrowest superconducting part in the load loop, which may be far less than half of the critical current of the tape before it is cut. The other more evident reason is that the circuit topology in the stacked tape is not as clear as that in a coil. There are mutual couplings between the 1st loop and the 2nd loop, as well as between the electromagnets and the 2nd loop. These mutual couplings generate significant loss. It is very difficult to further increase the maximum pumped current for a single stack without connecting it to external circuits.

However, the flux pumping technique requires only a small part of the HTS stack to be covered by external fields, which enables more compact magnetization setups to be made, and the separation of the HTS stack into a magnetization region and application region. As depicted by figure 13, a thick stack of HTS tapes can potentially be separated into a number of smaller stacks, to be magnetized individually with the flux pumps installed at their ends and the regions for trapped fields stacked together in the middle.

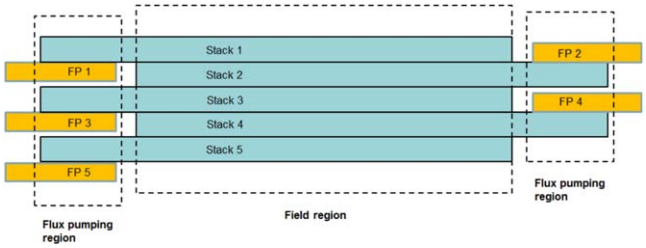

Figure 13. The proposed idea to magnetize a thick HTS stack with several flux pumps installed at the ends of each smaller stack, with each flux pump using much smaller fields than the full penetration field of the thick stack.

Separation of the magnetization can greatly reduce the cost and dimension of the magnetization setups, as generating a high magnitude field is much more difficult and costly than generating several fields of much smaller magnitudes.

6. Conclusion

This paper reports a new magnetization method for stacked HTS tapes: transformer–rectifier flux pumping. The experiments demonstrate this flux pumping method is effective in magnetizing the HTS stacks to a relatively decent level and is superior to the traveling-field flux pumping method for HTS stacks. The compactness of the setups and the potential to pump larger stacks makes this method promising for efficient *in situ* magnetization of superconducting PMs.

Acknowledgment

The authors would like to thank SuNam Co., Ltd for sponsoring the HTS coated conductors tapes used in this study.

ORCID iDs

Jianzhao Geng https://orcid.org/0000-0002-0808-8567

References

[1] Hull J and Murakami M 2004 Applications of bulk high-temperature superconductors *Proc. IEEE* **92** 1705–18
[2] Tomita M and Murakami M 2003 High-temperature superconductor bulk magnets that can trap magnetic fields of over 17 tesla at 29 K *Nature* **21** 517–20
[3] Durrell J *et al* 2014 A trapped field of 17.6 T in melt-processed, bulk Gd-Ba-Cu-O reinforced with shrink-fit steel *Supercond. Sci. Technol.* **27** 082001
[4] Wang J *et al* 2007 Laboratory-scale high temperature superconducting maglev launch system *IEEE Trans. Appl. Supercond.* **17** 2091–4
[5] Ma G *et al* 2008 Method to reduce levitation force decay of the bulk HTSC above the NdFeB guideway due to lateral movement *Supercond. Sci. Technol.* **21** 065020
[6] Coombs T A, Campbell A M, Storey R and Weller R 1999 Superconducting magnetic bearings for energy storage flywheels *IEEE Trans. Appl. Supercond.* **9** 968–71
[7] Jiang Y, Pei R, Xian W, Hong Z and Coombs T A 2008 The design, magnetization and control of a superconducting permanent magnet synchronous motor *Supercond. Sci. Technol.* **21** 065011
[8] Fuchs G *et al* 1999 Different limitations of trapped fields in melt-textured BCO *Applied Superconductivity 1999* vol 1 *(Sitges, Spain)* (Bristol: Institute of Physics Publishing) pp 111–4
[9] Vanderbemden P *et al* 2007 Remagnetization of bulk high-temperature superconductors subjected to crossed and rotating magnetic fields *Supercond. Sci. Technol.* **20** S174
[10] Hahn S, Kim S B, Ahn M C, Voccio J, Bascuñán J and Iwasa Y 2010 Trapped field characteristics of stacked YBCO thin plates for compact NMR magnets: spatial field distribution and temporal stability *IEEE Trans. Appl. Supercond.* **20** 1037–40
[11] Hahn S *et al* 2011 Field performance of an optimized stack of YBCO square 'Annuli' for a compact NMR magnet *IEEE Trans. Appl. Supercond.* **21** 1632–5
[12] Selva K and Majkic G 2013 Trapped magnetic field profiles of arrays of (Gd,Y)$Ba_2Cu_3O_x$ superconductor tape in different stacking configurations *Supercond. Sci. Technol.* **26** 115006
[13] Liu K *et al* 2018 Experimental studies on the dynamic responses of coated superconductor stack levitated above a permanent magnet guideway *IEEE Trans. Appl. Supercond.* **28** 3600305
[14] Patel A, Hopkins S C and Glowacki B A 2013 Trapped fields up to 2 T in a 12 mm square stack of commercial superconducting tape using pulsed field magnetization *Supercond. Sci. Technol.* **26** 032001
[15] Patel A, Filar K, Nizhankovskii V I, Hopkins S C and Glowacki B A 2013 Trapped fields greater than 7 T in a 12 mm square stack of commercial high-temperature superconducting tape *Appl. Phys. Lett.* **102** 102601
[16] Patel A, Baskys A, Mitchell-Williams T, McCaul A, Coniglio W, Hänisch J, Lao M and Glowacki B A 2017 A trapped field of 17.7 T in a stack of high temperature superconducting tape *Supercond. Sci. Technol.* **31** 09LT01
[17] Baghdadi M, Ruiz H S and Coombs T A 2014 Crossed-magnetic-field experiments on stacked second generation superconducting tapes: reduction of the demagnetization effects *Appl. Phys. Lett.* **104** 232602
[18] Bean C P 1964 Magnetization of high-field superconductors *Rev. Mod. Phys.* **36** 31
[19] Ainslie M D, Zhou D, Fujishiro H, Takahashi K, Shi Y-H and Durrell J H 2016 Flux jump-assisted pulsed field magnetisation of high-J_c bulk high-temperature superconductors *Supercond. Sci. Technol.* **29** 124004
[20] Coombs T A, Hong Z and Zhu X 2007 A thermally actuated superconducting flux pump *Physica* C **468** 153
[21] Hoffmann C, Pooke D and Flux A D 2011 Flux pump for HTS magnets *IEEE Trans. Appl. Supercond.* **21** 1628–31
[22] Walsh R M, Slade R, Pook D and Hoffmann C 2014 Characterization of current stability in an HTS NMR system energized by an HTS flux pump *IEEE Trans. Appl. Supercond.* **24** 4600805
[23] Jiang Z, Hamilton K, Amemiya N, Badcock R A and Bumby C W 2014 Dynamic resistance of a high-T_c superconducting flux pump *Appl. Phys. Lett.* **105** 112601
[24] Lee S *et al* 2016 Persistent current mode operation of a 2G HTS coil with a flux pump *IEEE Trans. Appl. Supercond.* **26** 0606104
[25] Zhang H *et al* 2017 Magnetization of coated conductor stacks using flux pumping *IEEE Trans. Appl. Supercond.* **27** 8200205

[26] Geng J and Coombs T A 2015 Mechanism of a high-T_c superconducting flux pump: using alternating magnetic field to trigger flux flow *Appl. Phys. Lett.* **107** 142601
[27] Andrianov V V, Zenkevich V B, Kurguzov V V, Sychev V V and Ternovskii F F 1970 *Sov. Phys. JETP* **31** 815
[28] Mikitik G P and Brandt E H 2001 Generation of a dc voltage by an ac magnetic field in type-II superconductors *Phys. Rev.* B **64** 092502
[29] Oomen M P, Rieger J, Leghissa M, ten Haken B and ten Kate H H 1999 Dynamic resistance in a slab-like superconductor with J_c(B) dependence *Supercond. Sci. Techno* **12** 382
[30] Jiang Z, Toyomoto R, Amemiya N, Zhang X and Bumby C W 2017 Dynamic resistance of a high-T_c coated conductor wire in a perpendicular magnetic field at 77 K *Supercond. Sci. Technol.* **30** 03LT01
[31] Geng J *et al* 2016 Origin of dc voltage in type II superconducting flux pumps: field, field rate of change, and current density dependence of resistivity *J. Phys. D: Appl. Phys.* **49** 11LT01
[32] Geng J, Matsuda K, Fu L, Shen B, Zhang X and Coombs T A 2016 Operational research on a high-T_c rectifier-type superconducting flux pump *Supercond. Sci. Technol.* **29** 035015
[33] Jiang Z *et al* 2018 Dynamic resistance measurement of a four-tape YBCO stack in a perpendicular magnetic field *IEEE Trans. Appl. Supercond.* **28** 8200305